Missing Mass Resolution in the Meson Spectroscopy Facility at CEBAF

Curtis A. Meyer

May 28, 1998

0.1 Resolution of the Detector

0.1.1 Introduction

In order to examine the response of the detector a simple momentum smearing has been employed. Final states are generated, and the momentum of the particles are smeared according to standard resolution functions.

0.1.2 Smearing of the beam Energy

It is assumed that in Stage 1 of the detector, simple endpoint tagging of the photon beam will be employed. This is currently what is done in the CLAS, and an energy resolution of 0.1% has been achieved. As such we use equation 1 to smear the incident photon energy. We have also assumed that the incident beam direction is know precisely.

$$\frac{\sigma_E}{E} = 0.001. \tag{1}$$

0.1.3 Smearing of the final state photons

Final state photons have their energy smeared according to equation 2. Where γ_s is a statistical fluctuation term, where its nominal value is $\gamma_s = 0.050$. The floor term, $\gamma_f = 0.020$ by default. Finally, it is assumed that in the case of the Pb–glass wall, the minimum detectable energy is $E_\gamma = 100MeV$.

$$\frac{\sigma_E}{E} = \frac{\gamma_s}{\sqrt{E}} + \gamma_f. \tag{2}$$

0.1.4 Smearing of charged particles

Charged particles are smeared according to standard formulae as given in equations 3, 4 and 5. In the case of the solenoidal field, it is assumed that we have a series of more–or–less equally spaced measurements. The transverse momentum, $p_\perp$ is determined from the curvature of the track in the $r\phi$ plane. The total momentum is determined from a measurement of the polar angle θ from r as a function of z. The latter is also affected by multiple scattering.

For a set of measurements with an $r\phi$ resolution σ_r, the resolution in $p_\perp$ is computed using equation 3. Where L_r is the radial distance from the first to the last hit and N is the number of measurements. In these studies, we will assume a nominal $\sigma_r = 200\mu m$. We will also assume that the innermost r measurement is at $r_i = 0.075m$ and that the maximum

measurement is at $r_o = 0.65m$. Depending on the angle θ, the outermost r may be smaller than the maximum. We also take a nominal value of $N = 10$.

$$\frac{\sigma_{p_\perp}}{p_\perp} = \frac{p_\perp \sigma_r}{eBL_r^2}\sqrt{\frac{720}{N+4}} \tag{3}$$

The error in θ is computed using equation 4 where σ_z is the resolution on the z–measurement and is nominally $0.002m$. L_z is the length in z from the first to last hit on the track, and N is the number of measurements, nominally $N = 10$. There is an assumption that the z measurement is significantly worse that the $r\phi$ measurement.

$$\sigma_\theta = \frac{\sigma_z}{L_z}\sqrt{\frac{12(N-1)}{N(N+1)}} \tag{4}$$

multiple scattering can also distort the θ measurement as given in equation 5. Here, L_s is the physical length of the track and X_0 is the radiation length of the material in the detector. Pure ethane would have $X_0 = 340m$.

$$\sigma_\theta = \frac{0.0136\sqrt{L_s/X_0}}{\beta p} \tag{5}$$

In the case of the dipole detector, it is assumed that the total momentum is measured with 0.5% accuracy, and that θ is measured exactly. Using the full 4.2m long LASS solenoid with the target approximately 1m in the magnet, tracks with θ larger than about 10° will reach the outermost radius of $r_o = 0.65m$ in equation 3. For these same tracks, the L_z in equation 4 will decrease as θ becomes larger.

The solenoid alone is capable of measuring tracks down to $\theta = 5°$. However, for tracks between 5° and 10° the radial and z lengths will be modified as: $L_r \approx 3.65 \tan\theta - 0.075$ and $L_z \approx 3.65 - r_i/\tan\theta$. This will lead to a fairly rapid deterioration of the momentum measurement. For angles smaller than about 7°, the dipole will take over, down to about 1°, with a fairly uniform momentum measurement.

0.2 Missing Mass Resolution

Of particular concern is being able to distinguish reactions of the form $\gamma p \to pX$ from $\gamma p \to \Delta X$. In particular, it is possible that the π from the decay of the baryon resonance, Δ may be missed by the detector. In order to study this, two reactions 6 and 7 have been simulated for $6GeV$, $8GeV$, $10GeV$ and $12GeV$ photon energy. In addition, X has been

generated as a $\Gamma = 0.150 GeV$ wide resonance of mass $1.7 GeV/c^2$, $2.5 GeV/c^2$ and $3.2 GeV/c^2$. In the case of 7, it has been assumed that the $\pi^\circ \to \gamma\gamma$ has been completely missed.

$$\gamma p \rightarrow p\left\{X \rightarrow \left[K^{*\circ} \rightarrow \pi^- K^+\right]\left[K^{*\circ} \rightarrow \pi^+ K^-\right]\right\} \quad (6)$$

$$\gamma p \rightarrow \left\{\Delta^+ \rightarrow [p\pi^\circ]\right\}\{X \rightarrow [K^* \rightarrow \pi K]\,[K^* \rightarrow \pi K]\} \quad (7)$$

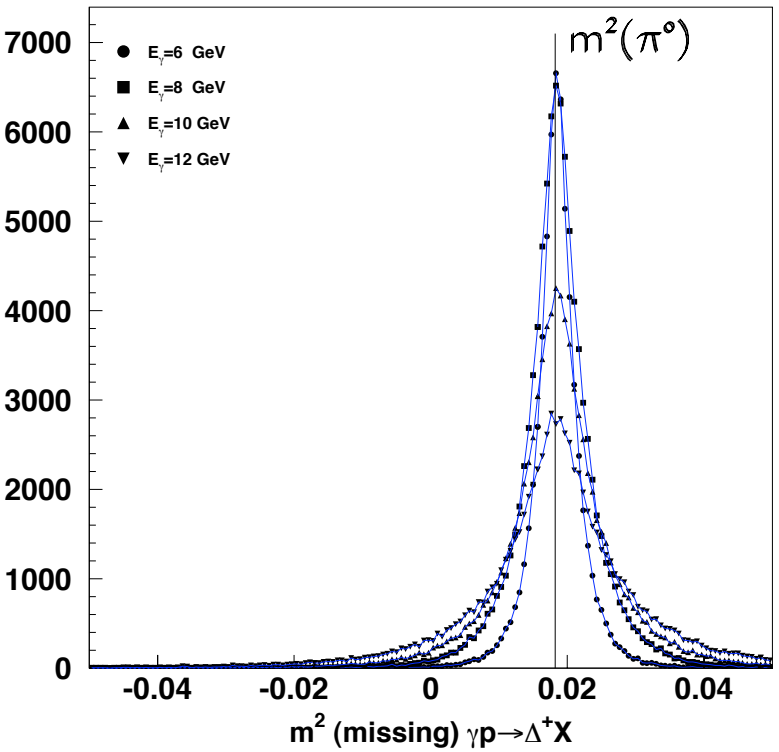

Figure 1: The missing–mass squared for a single π° under standard resolution assumptions in the solenoid only configuration. The reaction is $\gamma p \to \Delta^+ K^+ K^- \pi^+ \pi^-$ where the π° from the Δ^+ decay is not seen.

Figure 1 shows the missing mass with resolution for several different beam energies in the solenoid only configuration. Figure 2 shows the same plot in the solenoid plus dipole configuration. The important results of these plots are summarized in table 1 and table 2. First, the acceptance column indicates the fraction of events in which the five final state charged particles are detected, (K^+,K^-,π^+,π^- and p). In the solenoid–only mode, all particles

E_γ GeV	Acceptance		$m^2 < 0.005(GeV/c^2)^2$		$m^2 < 0.01(GeV/c^2)^2$	
6.0	61980/80000	0.775	323/61980	0.005	1356/61980	0.022
8.0	90943/120000	0.758	1814/90934	0.020	5610/90934	0.062
10.0	82878/120000	0.691	4502/82878	0.054	9612/82878	0.116
12.0	76769/120000	0.640	7959/76769	0.104	13709/76769	0.179

Table 1: Missing mass acceptance as a function of photon beam energy for the solenoid–only option. The *Acceptance* column requires that $\theta > 5^\circ$ for all charged particles. The < 0.005 requires that the missing–mass squared is smaller than $0.005(GeV/c^2)^2$, while the < 0.010 column requires that the missing–mass squared is smaller than $0.010(GeV/c^2)^2$.

must have $\theta_{\rm lab}$ larger than 5°. In the solenoid–dipole mode, the angular acceptance is increased down to about 1.5°, and significant increase in the acceptance is noted. In addition to this, we have assumed that all events in which the missing–masses squared is smaller than $0.005(GeV/c^2)^2$, ($m_m < .071 GeV/c^2$) would be misidentified as events without a missing π°. This fraction is reported as well as the fraction assuming the cut–off is $0.010(GeV/c^2)^2$, ($m_m < .100 GeV/c^2$). While the acceptance clearly improves with the addition of the dipole in all cases, the missing–mass resolution improves for the higher E_γ cases as well. This is due to the assumed 0.5% momentum resolution of the dipole all the way down to $\theta = 0^\circ$.

E_γ GeV	Acceptance		$m^2 < 0.005(GeV/c^2)^2$		$m^2 < 0.01(GeV/c^2)^2$	
6.0	77081/80000	0.964	575/77081	0.007	2150/77081	0.028
8.0	115396/120000	0.961	2520/115396	0.022	7369/115396	0.064
10.0	113858/120000	0.949	5550/113858	0.049	12435/113858	0.109
12.0	112710/120000	0.939	9696/112710	0.086	17795/112710	0.158

Table 2: Missing mass acceptance as a function of photon beam energy for the solenoid plus dipole option. The *Acceptance* column requires that $\theta > 1.5^\circ$ for all charged particles. The < 0.005 requires that the missing–mass squared is smaller than $0.005(GeV/c^2)^2$, while the < 0.010 column requires that the missing–mass squared is smaller than $0.010(GeV/c^2)^2$.

In addition to the dipole, we have also examined the effects of the various resolutions given in equations 3, 4 and 5. For these studies, we have taken $E_\gamma = 6GeV$ and looked at the effect of $\sigma_{r\phi}$, σ_z and X_0 on the missing–mass resolution. In Figure 3 is plotted the missing–mass squared as a function of $\sigma_{r\phi}$ for values from $100\mu m$ up to $900\mu m$. We have taken a value of $200\mu m$ as the default. Figure 4 shows the missing–mass squared as a function of σ_z for values from $1mm$ up to $9mm$. We have taken $2mm$ as the nominal value. In Figure 5 we plot

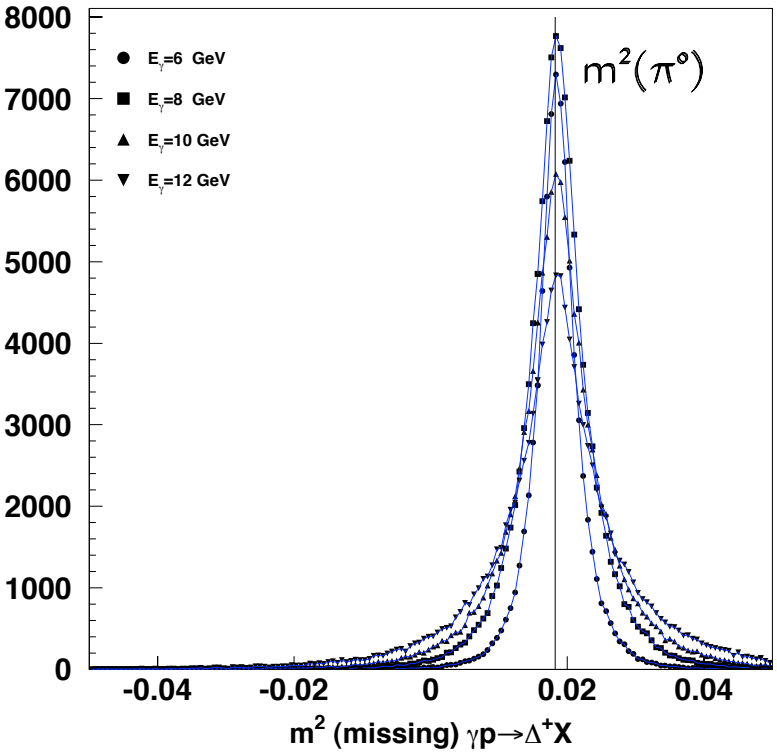

Figure 2: The missing–mass squared for a single π° under standard resolution assumptions in the solenoid plus dipole configuration. The reaction is $\gamma p \to \Delta^+ K^+ K^- \pi^+ \pi^-$ where the π° from the Δ^+ decay is not seen.

the missing–mass squared resolution as a function of the magnetic field strength from $0.50T$ up to $2.2T$, where the maximum field is $2.2T$. Finally, in Figure 6 is plotted the missing mass resolution as a function of the beam energy resolution.

Upon examining the missing–mass dependence on the various resolutions, we draw the following conclusions. The $200\mu m$ $r\phi$ resolution can not be allowed to deteriorate very much. There is some small gain as we improve it to $100\mu m$, but at least for the $6GeV$ case, that is not necessary. Similarly, we do not want the z resolution to get any worse than $2mm$, but these is not very much gain by improving things to $1mm$. The magnetic field could be operated at a lower setting, perhaps between $1T$ and $1.5T$ in the lowest beam energy configuration. Finally, the beam energy does not need to be known at a $0.001E_\gamma$ level, but it does need to be better than $0.0005E_\gamma$.

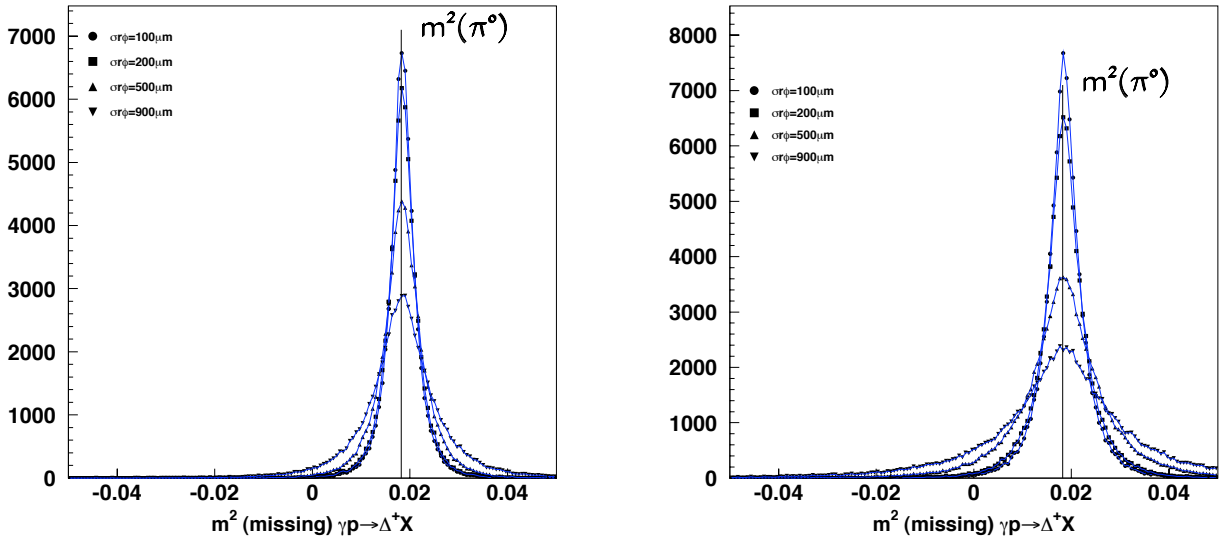

Figure 3: The missing–mass squared for a single π° in the solenoid only configuration. The left–hand plot is for a beam energy of $E_\gamma = 6GeV$, while the right–hand figure is for a beam energy of $E_\gamma = 8GeV$. The missing–mass squared is given as a function of $\sigma_{r\phi}$. The reaction is $\gamma p \to \Delta^+ K^+ K^- \pi^+ \pi^-$ where the π° from the Δ^+ decay is not seen.

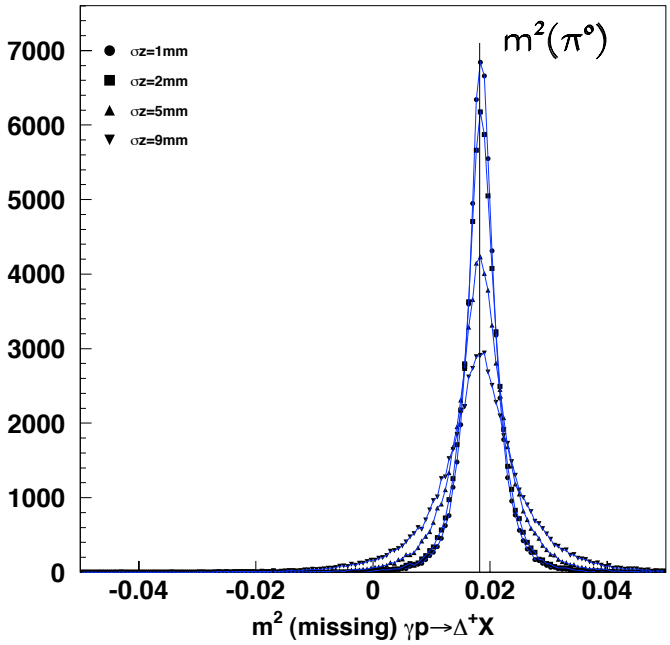

Figure 4: The missing–mass squared for a single π° for $E_\gamma = 6.GeV$ in the solenoid only configuration. The missing–mass squared is given as a function of σ_z. The reaction is $\gamma p \to \Delta^+ K^+ K^- \pi^+ \pi^-$ where the π° from the Δ^+ decay is not seen.

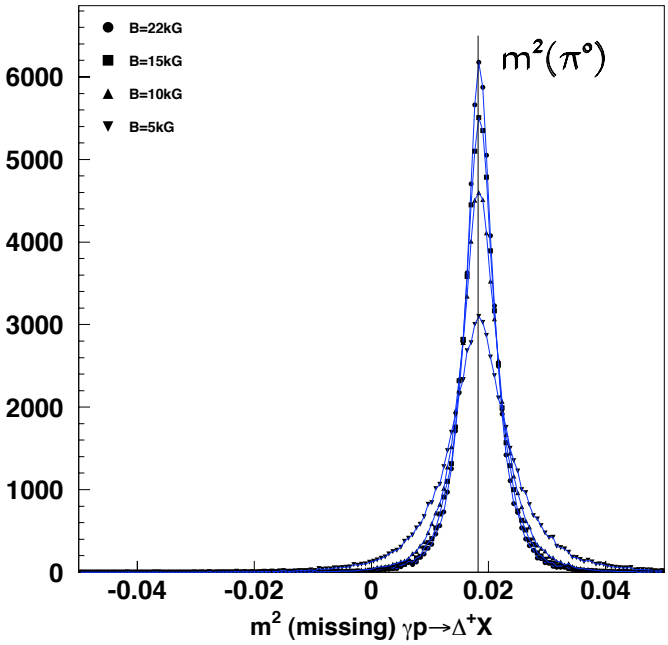

y

Figure 5: The missing–mass squared for a single π° for $E_\gamma = 6.GeV$ in the solenoid only configuration. The missing–mass squared is given as a function of magnetic field strength. The reaction is $\gamma p \to \Delta^+ K^+ K^- \pi^+ \pi^-$ where the π° from the Δ^+ decay is not seen.

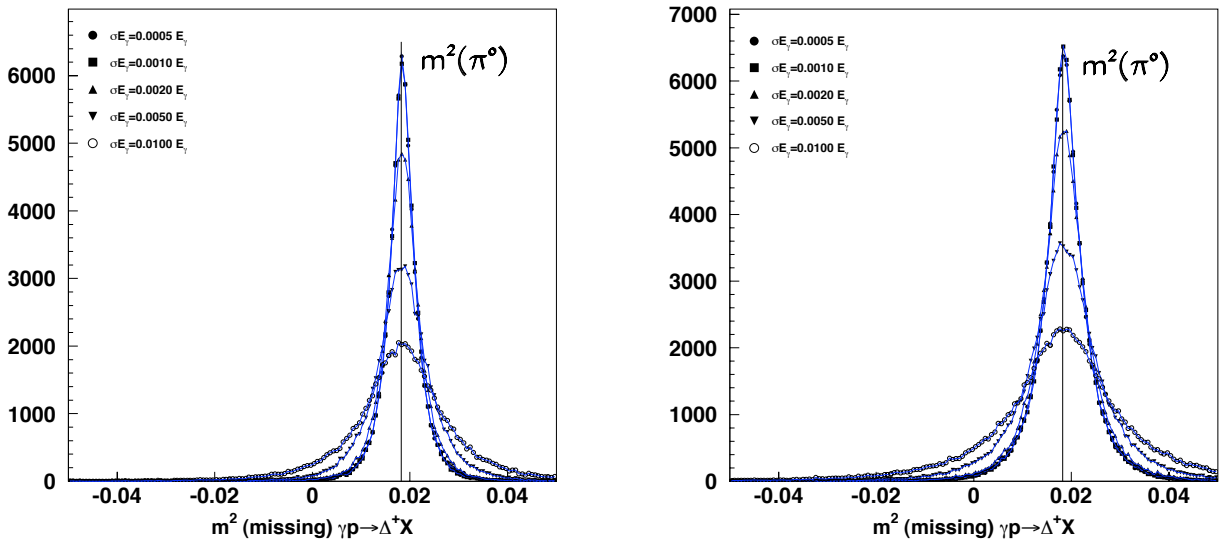

Figure 6: The missing–mass squared for a single π° in the solenoid only configuration. The left–hand plot is for a beam energy of $E_\gamma = 6GeV$ while the right–hand plot is for a beam energy of $E_\gamma = 8GeV$. The missing–mass squared is given as a function of the beam energy resolution. The reaction is $\gamma p \to \Delta^+ K^+ K^- \pi^+ \pi^-$ where the π° from the Δ^+ decay is not seen.

0.2.1 Inclusion of Photon Detection

All of the earlier discussion has assumed that we will be completely unable to detect the π° from the Δ decay. While this certainly allows to access certain aspects of the detector, in reality we will be able to detect some fraction of the π°'s, and certainly a class of events where we see one of the decay γ's. In table 3 are presented the fraction of photons detected under various configurations. The column *2 in Pb* indicate the fraction of events where both photons are measured in the Pb–glass detector. This tends to be small simply because the Pb–glass by itself covers very little solid angle. The most important number is *1 missed*, where one or both of the photons are completely missed. This number is dominated by the energy threshold in the crystals, rather than the solid angle coverage. In Figure 7 we show the photon energy spectrum for the four beam energies. The *inserts* show an expanded view of the 0 to 500MeV region, while the lines indicate where the 50MeV and 100MeV thresholds are. In Figure 8 we show a plot of θ_γ versus E_γ. The box along the bottom of the plot indicates the Pb–glass coverage, while the upper box shows the veto coverage, (This is artificially cut off at 2GeV). The dramatic feature is the narrow band in low energy along the left hand edge of these plots. Nearly all the missing photons are within the solid angle, they are simply below the energy threshold. In fact, lowering the energy threshold in the *veto* region would bring about the most dramatic increase in acceptance.

Beam Energy	*Photon Threshold*	*2 in Pb*	*1 in Pb 1 in veto*	*2 in Veto*	*1 missed*
$6.0GeV$	$100MeV$	0.046	0.212	0.328	0.414
$6.0GeV$	$50MeV$	0.046	0.258	0.527	0.168
$8.0GeV$	$100MeV$	0.070	0.214	0.346	0.370
$8.0GeV$	$50MeV$	0.070	0.257	0.518	0.155
$10.0GeV$	$100MeV$	0.084	0.201	0.356	0.359
$10.0GeV$	$50MeV$	0.085	0.241	0.524	0.150
$12.0GeV$	$100MeV$	0.105	0.181	0.385	0.329
$12.0GeV$	$50MeV$	0.106	0.218	0.539	0.137

Table 3: Fraction of photons detected for 6, 8, 10 and 12GeV beam energies with $100MeV$ and $50MeV$ photon thresholds in the detector system. The nominal design is for the solenoid only with photon veto inside the magnet.

There are two important conclusions from this section. It is extremely important to be able to detect, or at least veto photons in the veto region. It is also important to have as

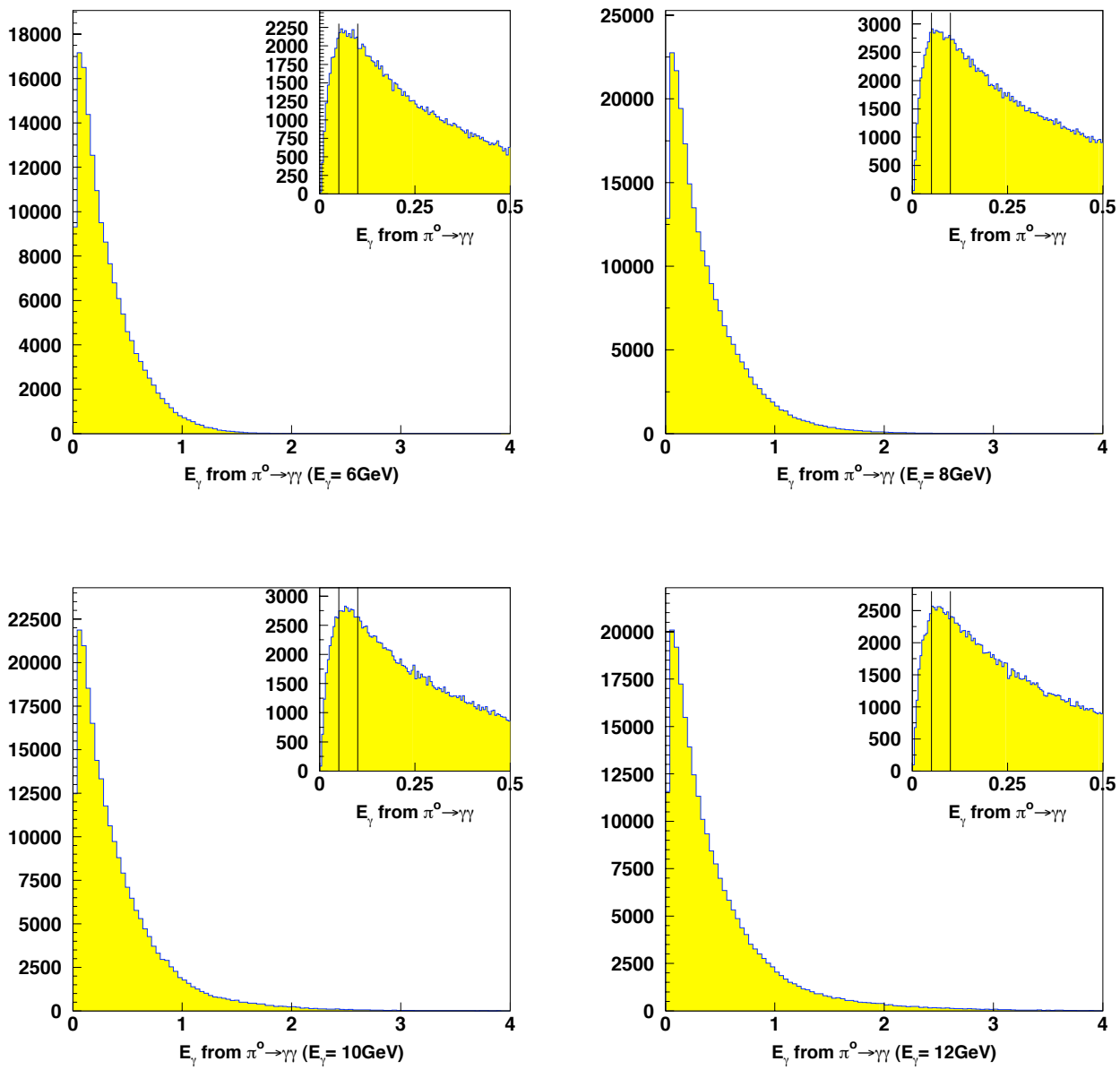

Figure 7: The photon energy spectrum from the π° decay from reaction 7. The four plots are for incident energies of 6, 8 10 and 12GeV. The insert shows an expanded view of the 0 to 500MeV photon energy region and the vertical lines indicate $E_\gamma = 100 MeV$.

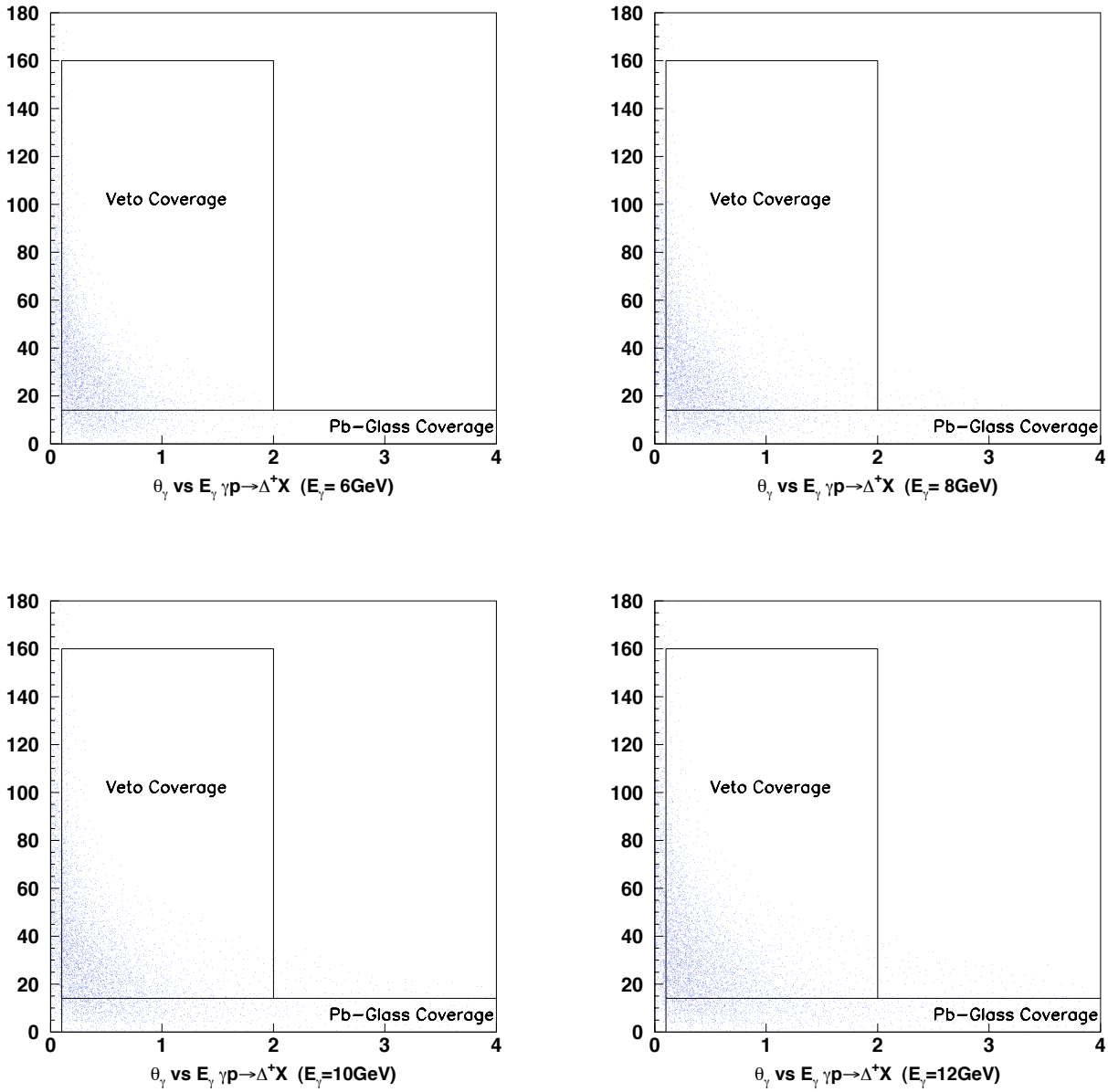

Figure 8: The photon angle versus photon energy from the π° decay from reaction 7. The four plots are for incident photon energies of 6, 8, 10 and 12GeV. The lower box indicates which photons are seen in the Pb–glass wall in the solenoid–only configuration. The upper box indicates which photons are seen in the veto detectors.

low an energy threshold as possible in the veto region.

References

[1] *Proceedings of the Workshop on Physics with 8+ GeV Photons*. July 14–15, 1997 Bloomington, IN.

[2] *Proceedings from the Jefferson Lab/NCSU Workshop on Hybrids and Photo production Physics*. November 13–15, 1997, Raleigh, NC.

[3] *Proceedings of the Physics with 8+ GeV Photons*. March 13–14, 1998, Pittsburgh, PA.

[4] D.Aston, *et al.*, *The LASS Spectrometer*, SLAC–Report–298, April 1986.